SIAM J. NUMER. ANAL.
Vol. 45, No. 5, pp. 2098–2119

HIGH-ORDER RELAXATION SCHEMES FOR NONLINEAR DEGENERATE DIFFUSION PROBLEMS*

FAUSTO CAVALLI†, GIOVANNI NALDI†, GABRIELLA PUPPO‡, AND MATTEO SEMPLICE†

Abstract. Several relaxation approximations to partial differential equations have been recently proposed. Examples include conservation laws, Hamilton–Jacobi equations, convection-diffusion problems, and gas dynamics problems. The present paper focuses on diffusive relaxation schemes for the numerical approximation of nonlinear parabolic equations. These schemes are based on a suitable semilinear hyperbolic system with relaxation terms. High-order methods are obtained by coupling ENO and weighted essentially nonoscillatory (WENO) schemes for space discretization with implicit-explicit (IMEX) schemes for time integration. Error estimates and a convergence analysis are developed for semidiscrete schemes with a numerical analysis for fully discrete relaxed schemes. Various numerical results in one and two dimensions illustrate the high accuracy and good properties of the proposed numerical schemes, also in the degenerate case. These schemes can be easily implemented on parallel computers and applied to more general systems of nonlinear parabolic equations in two- and three-dimensional cases.

Key words. parabolic problems, relaxation schemes, high-order accuracy, porous media equation, WENO reconstruction

AMS subject classifications. 65M20, 65M12, 35K65

DOI. 10.1137/060664872

1. Introduction. Relaxation approximations to nonlinear partial differential equations have been introduced in [22] (conservation laws) and [28] (degenerate diffusion) and later studied also in [2, 1, 21, 25, 29, 27]. The main idea is to approximate the original partial differential equation with a suitable semilinear hyperbolic system with stiff relaxation terms. As the relaxation parameter $\varepsilon \to 0$, the solution of the system converges to the solution of the original partial differential equation.

Moreover, appropriate numerical schemes for the relaxation system yield accurate numerical approximations to the original equation or system when the relaxation rate ϵ is sufficiently small. Numerically, the main advantage of solving the relaxation model over the original conservation law lies in the simple linear structure of characteristic fields and in the fact that the lower-order term is localized. In particular, the semilinear nature of the relaxation system gives a new way to develop numerical schemes that are simple, general, and Riemann solver free [20, 22].

The aim of this work is to analyze, from both a theoretical and a computational point of view, relaxation schemes for the numerical approximation of the following nonlinear degenerate diffusion problem:

$$\frac{\partial u}{\partial t} = D\Delta(p(u)), \quad x \in \mathbb{R}^d,\ t > 0, \tag{1.1}$$

with initial data $u(x,0) = u_0(x) \in L^1(\mathbb{R}^d)$. $D > 0$ is a diffusivity coefficient. As

*Received by the editors July 12, 2006; accepted for publication (in revised form) May 31, 2007; published electronically September 28, 2007. This work was partially supported by the MIUR/PRIN2005 project "Modellistica numerica per il calcolo scientifico ed applicazioni avanzate."
http://www.siam.org/journals/sinum/45-5/66487.html

†Dipartimento di Matematica, Università di Milano,Via Saldini 50, I-20133 Milano, Italy (cavalli@mat.unimi.it, giovanni.naldi@unimi.it, semplice@mat.unimi.it).

‡Dipartimento di Matematica, Politecnico di Torino, Corso Duca degli Abruzzi 24, 10129 Torino, Italy (gabriella.puppo@polito.it).

usual, we will assume $p : \mathbb{R} \to \mathbb{R}$ to be nondecreasing and Lipschitz continuous [36]. The equation is degenerate if $p(0) = 0$, and the set of points where $u(x)$ becomes 0 is called the interface.

In the case $p(u) = u^m$, $m > 1$, the previous equation is the *porous media equation*, which describes the flow of a gas through a porous interface according to some constitutive relation like Darcy's law in order to link the velocity of the gas and its pressure. With this choice of p, the diffusion coefficient mu^{m-1} vanishes at the points where $u = 0$. Thus the porous media equation is necessarily degenerate for compactly supported initial data [3], and the interfaces exhibit a finite speed of propagation. The degeneracy of the diffusion terms makes the dynamics of the interfaces difficult to study from both the theoretical and the numerical point of view. In general the numerical analysis of (1.2) is difficult for at least two reasons: the appearance of singularities for compactly supported solutions and the growth of the size of the support as time increases (*retention property*).

A common numerical technique to approximate (1.1) involves implicit discretization in time: It requires, at each time step, the solution of a nonlinear algebraic system, which can be singular on the interface. Another possibility is to linearize the nonlinear problem in order to take advantage of efficient linear solvers. For example, linear approximation schemes based on the so-called nonlinear Chernoff formula with a suitable relaxation parameter have been studied in [6, 26, 30, 31]. Other linear approximation schemes have been introduced by Jäger, Kačur, and Handlovičová [19, 23]. Also, a new scheme based on the maximum principle and on a perturbation and regularization approach was proposed by Pop and Yong in [33]. In the more general convection-diffusion case other approaches were investigated in the work of Evje and Karlsen [16], based on a suitable splitting of the convection and the diffusion operators, with a front tracking method for the advection term and implicit numerical integration of the latter. This approach limits the achievable order of accuracy and requires nonlinear solvers for the elliptic part.

A relaxation system to approximate degenerate parabolic equations was proposed originally in [28], inspired by kinetic schemes for the Carleman model. The convergence of the analytical solutions of the relaxation system to those of the partial differential equation is proven in [25], for the $u_t - (u^m)_{xx} = 0$ equation with $m > 0$ (porous media and fast-diffusion equations). The numerical integration of the relaxation system is performed at the macroscopic level, leading to the schemes proposed in [29, 27], where the kinetic derivation of the relaxation system is not relevant any more.

Natalini and coworkers proposed a kinetic approach to the numerical integration of conservation laws [2] and of convection-diffusion problems [7, 1]. Their work is based on a Bhatnagar–Gross–Krook (BGK) approximation which, despite being inspired by the work of Kurz and McKean as [28], is different at the kinetic level, as detailed in [24].

The aim of the present work is to obtain high-order numerical schemes in time and space for the integration of (1.1), following and developing the ideas of [27]. While in [27], the main focus is the development of suitable relaxation systems for several partial differential equations, here we will concentrate on the numerical analysis of the schemes resulting from the relaxation system. In particular we prove the convergence of the semidiscrete scheme, study the stability (linear and nonlinear) of the fully discrete scheme, and propose the construction of high-order extensions. In order to obtain higher-order methods, we couple ENO and weighted essentially nonoscillatory (WENO) schemes for space discretization and implicit-explicit (IMEX) schemes for time advancement. The schemes we obtain avoid both operator splitting techniques and implicit nonlinear solvers.

We point out that, despite the fact that high-order schemes may not reach their order of convergence due to the loss of regularity of the solution during the evolution, they are nevertheless interesting for error reduction when the number of grid points is fixed or until discontinuities develop (both cases arise, for example, in nonlinear filtering in image analysis [37]).

Note that the relaxation system we consider, following [27], can be obtained also as a three velocity model in the BGK approach of [24]. However, in the present case we are interested in the relaxed scheme, i.e., the $\varepsilon = 0$ limit of a numerical scheme for the relaxation system. For this reason, the numerical scheme we propose is different from those of [1], as described in the following section.

Our approach allows us to obtain numerical schemes for (1.1) that are easy to implement and suited for parallel coding, even in the multidimensional case and for more general and complex problems, such as oil recovery problems [15].

Equation (1.1) is a particular case of the more general convection diffusion equation

$$\frac{\partial u}{\partial t} + \operatorname{div} f(u) = D\Delta(p(u)), \quad x \in \mathbb{R}^d,\ t > 0. \tag{1.2}$$

The approach described in this paper can be extended to this more general case, introducing an additional equation to allow the relaxation of the convective term. However, this can be achieved in several ways, leading to different numerical schemes for the partial differential equation (1.2). The stability and efficiency of these schemes can differ wildly and will be the subject of further work [11].

The paper is organized as follows. Section 2 is devoted to the introduction of our relaxation schemes. The stability and error estimates of the semidiscrete scheme are provided in section 3. In section 4 we consider the fully discrete relaxed scheme with a nonlinear stability analysis and the extension to the multidimensional case. We also study parabolic problems in a bounded domain $\Omega \subset \mathbb{R}^d$ with Neumann boundary conditions. Finally, the implementation of the method as well as the results of several numerical experiments are discussed in section 5.

2. Relaxation approximation of nonlinear diffusion. The schemes proposed in the present work are based on the idea at the basis of the well-known relaxation schemes for hyperbolic conservation laws [22]. In the case of the nonlinear diffusion operator, an additional variable $\vec{v}(x,t) \in \mathbb{R}^d$ and a positive parameter ε are introduced, obtaining the following relaxation system:

$$\begin{cases} \dfrac{\partial u}{\partial t} + \operatorname{div}(\vec{v}) = 0, \\ \dfrac{\partial \vec{v}}{\partial t} + \dfrac{D}{\varepsilon}\nabla p(u) = -\dfrac{1}{\varepsilon}\vec{v}. \end{cases} \tag{2.1}$$

Formally, in the small relaxation limit, $\varepsilon \to 0^+$, system (2.1) approximates to leading order (1.1). Next, we remove the nonlinear term from the second equation, as in standard relaxation schemes, introducing a variable $w(x,t) \in \mathbb{R}$ and rewriting the system as:

$$\begin{cases} \dfrac{\partial u}{\partial t} + \operatorname{div}(\vec{v}) = 0, \\ \dfrac{\partial \vec{v}}{\partial t} + \dfrac{D}{\varepsilon}\nabla w = -\dfrac{1}{\varepsilon}\vec{v}, \\ \dfrac{\partial w}{\partial t} + \operatorname{div}(\vec{v}) = -\dfrac{1}{\varepsilon}(w - p(u)). \end{cases} \tag{2.2}$$

Formally, as $\varepsilon \to 0^+$, $w \to p(u)$, $v \to -D\nabla p(u)$, and the original diffusion equation (1.1) is recovered. As a matter of fact, this convergence can be justified rigorously by the results of section 3 of [7], since the relaxation system (2.2) can be seen as a particular case of the BGK system in [7]. Hence we are guaranteed that the solutions of (2.2) converge to the solutions of the degenerate parabolic equation when $\varepsilon \to 0^+$.

For the numerical integration of (2.2) one has to deal with the stiff characteristic velocities due to the term $\nabla(w)/\varepsilon$. In [1], the authors propose two possible methods: either choose ε dependent of the space discretization h or consider $\varepsilon = 0$ and use a splitting technique. Instead, we introduce a suitable parameter φ and rewrite the system (2.2) as

$$\begin{cases} \dfrac{\partial u}{\partial t} + \operatorname{div}(\vec{v}) = 0, \\ \dfrac{\partial \vec{v}}{\partial t} + \varphi^2 \nabla w = -\dfrac{1}{\varepsilon}\vec{v} + \left(\varphi^2 - \dfrac{D}{\varepsilon}\right)\nabla w, \\ \dfrac{\partial w}{\partial t} + \operatorname{div}(\vec{v}) = -\dfrac{1}{\varepsilon}(w - p(u)). \end{cases} \tag{2.3}$$

We anticipate here that we intend to integrate implicitly the terms on the right-hand side of system (2.3), so that we can consider the case $\varepsilon = 0$ without being limited by the stiffness of the problem. In particular, in the relaxed case (i.e., $\varepsilon = 0$), the stiff source terms can be integrated by solving a system that is already in a suitable triangular form and does not require iterative solvers.

In the previous system the parameter ε has physical dimensions of time and represents the so-called relaxation time. Furthermore, w has the same dimensions as u, while each component of $\vec{v}$ has the dimension of u times a velocity; finally φ is a velocity. The inverse of ε gives the rate at which v decays onto $-\nabla p(u)$ in the evolution of the variable $\vec{v}$ governed by the stiff second equation of (2.3).

Equations (2.3) form a semilinear hyperbolic system with a stiff source term. The characteristic velocities of the hyperbolic part are given by $0, \pm\varphi$. The parameter φ allows one to "move" the stiff terms $\frac{D}{\varepsilon}\nabla p(u)$ to the right-hand side, without losing the hyperbolicity of the system.

We point out that degenerate parabolic equations often model physical situations with free boundaries or discontinuities: We expect that schemes for hyperbolic systems will be able to reproduce faithfully these details of the solution. One of the main properties of (2.3) consists in the semilinearity of the system; that is, all of the nonlinearities are in the (stiff) source terms, while the differential operator is linear. Hence, the solution of the convective part requires neither Riemann solvers nor the computation of the characteristic structure at each time step, since the eigenstructure of the system is constant in time. Moreover, the relaxation approximation does not exploit the form of the nonlinear function p, and hence it gives rise to a numerical scheme that, to a large extent, is independent of it, resulting in a very versatile tool.

3. The semidiscrete scheme. System (2.3) can be written in the form:

$$z_t + \operatorname{div} f(z) = \frac{1}{\varepsilon} g(z), \tag{3.1}$$

where

$$z = \begin{pmatrix} u \\ v \\ w \end{pmatrix}, \qquad f(z) = \begin{bmatrix} v^T \\ \Phi^2 w \\ v^T \end{bmatrix}, \qquad g(z) = \begin{pmatrix} 0 \\ -v + (\varphi^2\varepsilon - D)\nabla w \\ p(u) - w \end{pmatrix}, \tag{3.2}$$

and Φ^2 is the $d \times d$ identity matrix times the scalar φ^2. We start discretizing the system in time using, for simplicity, a uniform time step Δt. Let $z^n(x) = z(x, t^n)$, with $t^n = n\Delta t$. Since (3.1) involves both stiff and nonstiff terms, it is a natural idea to employ different time-discretization strategies for each of them, as in [4, 32]. In this work we integrate (3.1) with a Runge–Kutta IMEX scheme [32], obtaining the following semidiscrete formulation:

$$z^{n+1} = z^n - \Delta t \sum_{i=1}^{\nu} \tilde{b}_i \mathrm{div} f(z^{(i)}) + \frac{\Delta t}{\varepsilon} \sum_{i=1}^{\nu} b_i g(z^{(i)}), \tag{3.3}$$

where the $z^{(i)}$'s are the stage values of the Runge–Kutta scheme which are given by

$$z^{(i)} = z^n - \Delta t \sum_{k=1}^{i-1} \tilde{a}_{i,k} \mathrm{div} f(z^{(k)}) + \frac{\Delta t}{\varepsilon} \sum_{k=1}^{i} a_{i,k} g(z^{(k)}), \tag{3.4}$$

where $\tilde{b}_i$, $\tilde{a}_{ij}$ and b_i, a_{ij} denote the coefficients of the explicit and implicit Runge–Kutta schemes, respectively. We assume that the implicit scheme is of the diagonally implicit type. To find the $z^{(i)}$'s it is necessary in principle to solve a nonlinear system of equations which, however, can be easily decoupled. The system for the first stage $z^{(1)}$ at time t^n is

$$\begin{pmatrix} u^{(1)} \\ v^{(1)} \\ w^{(1)} \end{pmatrix} = \begin{pmatrix} u^n \\ v^n \\ w^n \end{pmatrix} + \frac{\Delta t}{\varepsilon} a_{11} \begin{pmatrix} 0 \\ -v^{(1)} + (\varphi^2\varepsilon - D)\nabla w^{(1)} \\ p(u^{(1)}) - w^{(1)} \end{pmatrix}. \tag{3.5}$$

The first equation yields $u^{(1)} = u^n$; substituting in the third equation, we immediately find $w^{(1)}$; and finally, substituting $w^{(1)}$ in the second equation, we compute $v^{(1)}$. In other words, the system can be written in triangular form. For the following stage values, by grouping the already computed terms in the vector $B^{(i)}$ given by

$$B^{(i)} = z^n - \Delta t \sum_{k=1}^{i-1} \tilde{a}_{i,k} \mathrm{div} f(z^{(k)}) + \frac{\Delta t}{\varepsilon} \sum_{k=1}^{i-1} a_{i,k} g(z^{(k)}), \tag{3.6}$$

the new stage values are given by

$$\begin{pmatrix} u^{(i)} \\ v^{(i)} \\ w^{(i)} \end{pmatrix} = B^{(i)} + \frac{\Delta t}{\varepsilon} a_{ii} \begin{pmatrix} 0 \\ -v^{(i)} + (\varphi^2\varepsilon - D)\nabla w^{(i)} \\ p(u^{(i)}) - w^{(i)} \end{pmatrix}, \tag{3.7}$$

which is again a triangular system. In the numerical tests, we will apply IMEX schemes of order 1, 2, and 3.

Following [22] we set $\varepsilon = 0$, thus obtaining the so-called *relaxed scheme*. The computation of the first stage reduces to

$$\begin{aligned} u^{(1)} &= u^n, \\ w^{(1)} &= p(u^{(1)}), \\ v^{(1)} &= -D\nabla w^{(1)}. \end{aligned} \tag{3.8}$$

For the following stages the first equation is

$$u^{(i)} = u^n - \Delta t \sum_{k=1}^{i-1} \tilde{a}_{i,k} \mathrm{div} v^{(k)}. \tag{3.9}$$

In the other equations the convective terms are dominated by the source terms, and thus $v^{(i)}$ and $w^{(i)}$ are given by

$$\begin{aligned} v^{(i)} &= -D \nabla w^{(i)}, \\ w^{(i)} &= p(u^{(i)}). \end{aligned} \tag{3.10}$$

We see that only the explicit part of the Runge–Kutta method is involved in the updating of the solution. Then, in the relaxed schemes we use only the explicit part of the tableaux. In particular we consider second- and third-order strongly stable Runge–Kutta (SSRK) schemes [17], namely,

`IMEX1` (1^{st} order) `IMEX2` (2^{nd} order) `IMEX3` (3^{rd} order)

0	
1	

0	0	
1	0	
$\frac{1}{2}$	$\frac{1}{2}$	

0	0	0	
1	0	0	
$\frac{1}{4}$	$\frac{1}{4}$	0	
$\frac{1}{6}$	$\frac{1}{6}$	$\frac{2}{3}$	

In [10] we studied the increase in efficiency obtained by using suitable strongly stable Runge–Kutta schemes.

3.1. Convergence of the semidiscrete relaxed scheme. The aim of this section is to show the L^1 convergence of the solution of the semidiscrete in time relaxed scheme defined by (3.8), (3.9), and (3.10). We will extend the theorem proved in [6], where only the case of forward Euler time stepping was considered. In this section, for the sake of simplicity, we set $D = 1$.

Theorem 3.1 proves that the numerical solution of the relaxed scheme converges to the solution of (1.1). The proof does not make explicit use of the convergence of the solutions of the relaxation system (2.3) to the solutions of (1.1).

Eliminating v from (3.8) and (3.9) using (3.10), we rewrite the relaxed scheme as

$$\begin{aligned} u^{(1)} &= u^n, \\ w^{(1)} &= p(u^n) \end{aligned} \tag{3.11}$$

for the first stage, and

$$\begin{aligned} u^{(i)} &= u^n + \Delta t \sum_{k=1}^{i-1} \tilde{a}_{i,k} \Delta w^{(k)}, \\ w^{(i)} &= p(u^{(i)}) \end{aligned} \tag{3.12}$$

for subsequent stages. We recall that a Runge–Kutta scheme for the ordinary differential equation $y' = R(y)$ can also be written in the form [17]

$$\begin{aligned} y^{(1)} &= y^n, \\ y^{(i)} &= \sum_{k=1}^{i-1} \alpha_{ik} \left(y^{(k)} + \Delta t \frac{\beta_{ik}}{\alpha_{ik}} R(y^{(k)}) \right), \qquad i = 2, \ldots, \nu, \end{aligned} \tag{3.13}$$

where $y^{n+1} = y^{(\nu)}$. For consistency, $\sum_{k=1}^{i-1} \alpha_{ik} = 1$ for every $i = 1, \ldots, \nu$. Moreover we assumed that $\alpha_{ik} \geq 0$ and $\beta_{ik} \geq 0$ and that $\alpha_{ik} = 0$ implies $\beta_{ik} = 0$. Under these assumptions, each stage value $y^{(i)}$ can be written as a convex combination of forward Euler steps. This remark allows us to study the convergence of the Runge–Kutta scheme in terms of the convergence of the explicit forward Euler scheme applied to the nonlinear diffusion problem.

This latter was studied in [6] via a nonlinear semigroup argument. In the following we review the approach of [6], and next we extend the proof to the case of a ν-stages explicit Runge–Kutta scheme.

3.1.1. The forward Euler case. We wish to solve the evolution equation

$$\frac{du}{dt} + Lp(u) = 0, \qquad u(\cdot, t = 0) = u_0, \tag{3.14}$$

on the domain Ω, where $L = -\Delta$ and $p : \mathbb{R} \to \mathbb{R}$ is a nondecreasing locally Lipschitz function such that $p(0) = 0$. Under these hypotheses, the nonlinear operator $Au = Lp(u)$ with domain $D(A) = \{u \in L^1(\Omega) : p(u) \in D(L)\}$ is m-accretive in $L^1(\Omega)$; that is, for all $\varphi \in \mathrm{L}^1(\Omega)$ and for all $\lambda > 0$ there exists a unique solution $u \in D(A)$ such that $u + \lambda Lp(u) = \varphi$ and the application defined by $\varphi \mapsto u$ is a contraction [14].

Moreover $D(A)$ is dense in $L^1(\Omega)$, so it follows that

$$S_A(t)u_0 = \lim_{m\to\infty} \left(\mathbb{I} + \frac{t}{m}A\right)^{-m} u_0 \tag{3.15}$$

is a contraction semigroup on $L^1(\Omega)$ and $S_A(t)u_0$ is the generalized solution of (3.14) in the sense of Crandall–Liggett [14]. Let $S(t)$ be the linear contraction semigroup generated by $-L$; that is, $u(t) = S(t)u_0$ is the solution of the initial value problem $u_t = -L(u)$ and $u(\cdot, t = 0) = u_0$. The algorithm proposed in [6] is

$$\frac{u^{n+1} - u^n}{\tau} + \left[\frac{\mathbb{I} - S(\sigma_\tau)}{\sigma_\tau}\right] p(u^n) = 0, \tag{3.16}$$

where τ is the time step and $\sigma_\tau \downarrow 0$. This can be written as

$$u^{n+1} = F_E(\tau)u^n, \quad \text{where } F_E(\tau)\varphi = \varphi + \frac{\tau}{\sigma_\tau}\left[S(\sigma_\tau) - \mathbb{I}\right] p(\varphi). \tag{3.17}$$

Hence

$$u^n = (F_E(\tau))^n u_0. \tag{3.18}$$

The proof in [6] is based on the following argument. Note that formally $S(\sigma_\tau)\varphi \sim e^{-\sigma_\tau L}\varphi$. Let $t = \tau n$ and

$$\begin{aligned} u(t) &= \left[\mathbb{I} + \frac{t}{n\sigma_\tau}\left(S(\sigma_\tau) - \mathbb{I}\right) \circ p\right]^n u_0 \\ &= \left[\mathbb{I} + \frac{t}{n\sigma_\tau}\left(e^{-\sigma_\tau L} - \mathbb{I}\right) \circ p\right]^n u_0 \qquad \text{if } \sigma_\tau \to 0 \\ &= \left[\mathbb{I} - \frac{t}{n} L \circ p\right]^n u_0 \\ &\to S_A(u_0) \qquad \text{when } n \to \infty. \end{aligned} \tag{3.19}$$

The convergence proof requires that $\mu\frac{\tau}{\sigma_\tau} \leq 1$, where μ is the Lipschitz constant of $p(u)$. We point out that σ_τ is linked to the spatial approximation of the operator L, and in our scheme this requirement is reflected in the stability condition of the fully discrete scheme (see section 4).

3.1.2. Runge–Kutta schemes. Now we are going to prove convergence for the case of a ν-stages Runge–Kutta scheme.

Let $t > 0$ and $\tau = t/n$, with $n \geq 1$; let $\sigma_\tau : (0,\infty) \to (0,\infty)$ be a function such that $\lim_{\tau\to 0} \sigma_\tau = 0$.

$$\begin{aligned} &u^{(1)} = u^n, \\ &u^{(i)} = \sum_{k=1}^{i-1} \alpha_{ik} \left[u^{(k)} + \tau \frac{\beta_{ik}}{\alpha_{ik}} A(u^{(k)}) \right], \qquad i = 2, \dots, \nu, \end{aligned} \tag{3.20}$$

and proceeding as in (3.19), this becomes

$$\begin{aligned} &u^{(1)} = u^n, \\ &u^{(i)} = \sum_{k=1}^{i-1} \alpha_{ik} \left[u^{(k)} + \tau \frac{\beta_{ik}}{\alpha_{ik}} (S(\sigma_\tau) - \mathbb{I}) \circ p(u^{(k)}) \right], \qquad i = 2, \dots, \nu, \\ &u^{n+1} = u^{(\nu)}. \end{aligned} \tag{3.21}$$

We now extend (3.17) to the Runge–Kutta scheme defined by (3.21). Define, for $\phi \in L^1(\Omega)$,

$$\begin{aligned} &F^{(1)}(\tau)\phi = \phi, \\ &F^{(i)}(\tau)\phi = \sum_{k=1}^{i-1} \alpha_{ik} F^{(k)}(\tau)\phi + \frac{\tau\beta_{ik}}{\sigma_\tau} \left[S(\sigma_\tau) - \mathbb{I} \right] p(F^{(k)}(\tau)\phi), \\ &F(\tau)\phi = F^{(\nu)}(\tau)\phi, \end{aligned} \tag{3.22}$$

and therefore

$$u^n(t) = [F(\tau)]^n u_0. \tag{3.23}$$

Let $u(t)$ be the generalized solution of (3.14). The following theorem proves the convergence of the semidiscrete solution to $u(t)$.

THEOREM 3.1. *Assume $u^0 \in L^\infty(\Omega)$, and $\|u^0\|_\infty = M$; let p be a nondecreasing Lipschitz continuous function on $[-M, M]$ with Lipschitz constant μ. Assume that the following conditions hold:*

$$\begin{cases} \alpha_{ik} \geq 0, \\ \beta_{ik} \geq 0, \\ \alpha_{ik} = 0 \Rightarrow \beta_{ik} = 0, \\ \displaystyle\sum_{k=1}^{i-1} \alpha_{ik} = 1 \ \textit{(consistency)}, \\ \dfrac{\mu\tau}{\sigma_\tau} \leq \min \dfrac{\alpha_{ik}}{\beta_{ik}} \quad \textit{for } \tau > 0, \alpha_{ik} \neq 0 \qquad \textit{(stability)}, \end{cases} \tag{3.24}$$

and then $\lim_{n\to\infty} u^n(t) = u(t)$ in L^1. Moreover the convergence is uniform for t in any given bounded interval.

The proof follows the steps of [6]: First we show that u^n verifies a maximum principle (Lemma 3.2) and that F is a contraction (Lemma 3.3), and finally we apply the nonlinear Chernoff formula [8].

LEMMA 3.2. *If* (3.24) *is verified, then* $-M \le u^n \le M$ *for all* n.

Proof. We argue by induction on n: We assume that $-M \le u^n \le M$, and we show that $-M \le u^{n+1} \le M$. Let

$$u^{(i)} = F^{(i)}(\tau)u^n. \tag{3.25}$$

Since $u^{n+1} = u^{(\nu)}$, it suffices to prove that $-M \le u^{(i)} \le M$ for $i = 1, \dots, \nu$. We prove this by induction on i. When $i = 1$, the statement is true thanks to the induction hypothesis on n and being $F^{(1)} = \mathbb{I}$. Let's assume that $-M \le u^{(i-1)} \le M$ holds; we are going to show that

$$-M \le u^{(i)} = F^{(i)}(\tau)u^n \le M. \tag{3.26}$$

The function $s \mapsto \alpha_{ik}s - \frac{\tau\beta_{ik}}{\sigma_\tau}p(s)$ is nondecreasing thanks to (3.24) and the hypotheses on the function p. By the induction hypothesis on i, we have that for $k = 1, \dots, i-1$

$$-\alpha_{ik}M - \frac{\tau\beta_{ik}}{\sigma_\tau}p(-M) \le \alpha_{ik}u^{(k)} - \frac{\tau\beta_{ik}}{\sigma_\tau}p(u^{(k)}) \le \alpha_{ik}M - \frac{\tau\beta_{ik}}{\sigma_\tau}p(M). \tag{3.27}$$

Using again the induction hypothesis on i and recalling that p is nondecreasing, since S is a contraction in L^∞ [6] and $p(-M) \le p(u^{(k)}) \le p(M)$,

$$p(-M) \le S\left(p(u^{(k)})\right) \le p(M). \tag{3.28}$$

Multiplying the last equation by $\frac{\tau\beta_{ik}}{\sigma_\tau}$ and summing it to (3.27), we get

$$-\alpha_{ik}M \le \alpha_{ik}u^{(k)} + \frac{\tau\beta_{ik}}{\sigma_\tau}(S - \mathbb{I})p(u^{(k)}) \le \alpha_{ik}M, \qquad k = 1, \dots, i-1. \tag{3.29}$$

Summing for $k = 1, \dots, i-1$ and using the consistency relation of (3.24):

$$-M \le \sum_{k=1}^{i-1} \alpha_{ik}u^{(k)} + \frac{\tau\beta_{ik}}{\sigma_\tau}(S - \mathbb{I})p(u^{(k)}) \le M. \tag{3.30}$$

In particular this is valid when $i = \nu$, proving that $-M \le u^{(n+1)} \le M$. ∎

Now we can replace p by $\overline{p}$, where $\overline{p} = p$ in $-M \le x \le M$, $\overline{p} = p(M)$ for $x \ge M$, and $\overline{p} = p(-M)$ for $x \le -M$: The algorithm is the same, and in what follows we can assume that p is Lipschitz continuous with constant μ on all $\mathbb{R}$.

LEMMA 3.3. *If the hypotheses of Theorem* 3.1 *hold, then* $F(\tau)$ *is a contraction on* $L^1(\Omega)$, *i.e.,*

$$\|F(\tau)\phi - F(\tau)\psi\|_1 \le \|\phi - \psi\|_1 \qquad \forall \psi, \phi \in L^1. \tag{3.31}$$

Proof. We start showing that the result holds for a single forward Euler step. Recalling the definition of F_E from (3.17)

$$\begin{aligned} \|F_E(\tau)\phi - F_E(\tau)\psi\|_1 &\le \frac{\tau}{\sigma_\tau}\left\|S(\sigma_\tau)[p(\phi) - p(\psi)]\right\|_1 + \left\|(\phi - \psi) - \frac{\tau}{\sigma_\tau}[p(\phi) - p(\psi)]\right\|_1 \\ &\le \frac{\tau}{\sigma_\tau}\left\|p(\phi) - p(\psi)\right\|_1 + \left\|\left(\phi - \frac{\tau}{\sigma_\tau}p(\phi)\right) - \left(\psi - \frac{\tau}{\sigma_\tau}p(\psi)\right)\right\|_1 \\ &= \left\|\phi - \psi\right\|_1, \end{aligned} \tag{3.32}$$

where we used the contractivity of S. The last equality relies on the fact that p and the function $x \mapsto x - \frac{\tau}{\sigma_\tau} p(x)$ are nondecreasing, which in turn is guaranteed by the stability condition, which in this case reduces to $\mu\tau/\sigma_\tau \leq 1$ [6].

In the general case we have

$$\begin{aligned} \|F^{(i)}(\tau)\phi - F^{(i)}(\tau)\psi\|_1 &\leq \sum_{k=1}^{i-1} \alpha_{ik} \left\| F_E\left(\frac{\tau\beta_{ik}}{\alpha_{ik}}\right) F^{(k)}(\tau)\phi - F_E\left(\frac{\tau\beta_{ik}}{\alpha_{ik}}\right) F^{(k)}(\tau)\psi \right\|_1 \\ &\leq \sum_{k=1}^{i-1} \alpha_{ik} \left\| F^{(k)}(\tau)\phi - F^{(k)}(\tau)\psi \right\|_1 \qquad (3.33) \\ &\leq \|\phi - \psi\|_1 . \end{aligned}$$

In the second inequality we used the contractivity of F_E and the stability condition, while in the third one we apply an induction argument on the contractivity of $F^{(k)}$, the positivity constraint on α_{ik} and β_{ik}, as well as the consistency condition $\sum_k \alpha_{ik} = 1$. Setting $i = \nu$ yields the result. ∎

Proof of Theorem 3.1. Let ψ_τ and ψ be, respectively,

$$\psi_\tau = \left(I + \frac{\lambda}{\tau}(I - F(\tau))\right)^{-1} \phi \qquad \text{and} \qquad \psi = (I + \lambda A)^{-1}\phi. \qquad (3.34)$$

The function ψ exists since the operator A is m-accretive, whereas the existence of the function ψ_τ is guaranteed by the following fixed-point argument. Let

$$G(y) = \frac{1}{1+\eta}\phi + \frac{\eta}{\eta+1} F(\tau) y,$$

where $\phi \in \mathrm{L}^1$, $y \in \overline{D(A)}$, and $\eta \geq 0$. We have

$$\|G(y) - G(x)\| = \frac{\eta}{\eta+1}\|F(\tau)y - F(\tau)x\| \leq \frac{\eta}{\eta+1}\|y - x\|$$

since F is a contraction, as proved in Lemma 3.3. Thus G is also a contraction, and therefore it possesses a unique fixed point which coincides with ψ_τ.

We want to show that

$$\psi_\tau \to \psi \qquad \text{in } \mathrm{L}^1$$

as $\tau \to 0$ for each fixed $\lambda > 0$. Let

$$\phi_\tau = \psi + \frac{\lambda}{\tau}(\mathbb{I} - F(\tau))\psi.$$

We want to estimate $\psi_\tau - \psi$ in terms of $\phi_\tau - \phi$.

$$\phi_\tau - \phi = \left(1 + \frac{\lambda}{\tau}\right)(\psi - \psi_\tau) - \frac{\lambda}{\tau}(F(\tau)\psi - F(\tau)\psi_\tau),$$

Therefore

$$\left(1 + \frac{\lambda}{\tau}\right)(\psi - \psi_\tau) - (\phi_\tau - \phi) = \frac{\lambda}{\tau}(F(\tau)\psi - F(\tau)\psi_\tau),$$

and, by taking norms and using the fact that F is a contraction, we have

$$\left|\left(1+\frac{\lambda}{\tau}\right)\|\psi-\psi_\tau\|-\|\phi_\tau-\phi\|\right| \le \left\|\left(1+\frac{\lambda}{\tau}\right)(\psi-\psi_\tau)-(\phi_\tau-\phi)\right\| \le \frac{\lambda}{\tau}\|\psi-\psi_\tau\|.$$

In particular

$$\left(1+\frac{\lambda}{\tau}\right)\|\psi-\psi_\tau\|-\|\phi_\tau-\phi\| \le \frac{\lambda}{\tau}\|\psi-\psi_\tau\|,$$

and therefore $\|\psi-\psi_\tau\| \le \|\phi-\phi_\tau\|$.

Now we estimate $\|\phi-\phi_\tau\|$ in the simple case of a forward Euler scheme. Note that

$$\phi-\phi_\tau = \lambda A\psi - \frac{\lambda}{\tau}(\mathbb{I}-F(\tau))\psi,$$

and thus $\|\phi-\phi_\tau\|$ measures a sort of consistency error. For a single forward Euler step, $F=F_E$, where F_E is defined in (3.17). Thus

$$\|\phi-\phi_\tau\| = \lambda\left\|A\psi-\frac{1}{\sigma_\tau}(\mathbb{I}-S(\sigma_\tau))p(\psi)\right\| \to 0 \tag{3.35}$$

as $\tau\to 0$ since $\frac{\mathbb{I}-S(\sigma_\tau)}{\sigma_\tau}p(\psi)\to Lp(\psi)=A\psi$.

The more general case of a ν-stages Runge–Kutta scheme can be carried out by induction following the procedure already applied in the proofs of the previous lemmas.

We now use Theorem 3.2 of [8], which, specialized to our case, can be written as follows. Assume that $F(\tau):\mathrm{L}^1\to\mathrm{L}^1$ for $\tau>0$ is a family of contractions. Assume further that an m-accretive operator A is given, and let $S(t)$ be the semigroup generated by A. Assume further that the family $F(\tau)$ and the operator A are linked by the following formula:

$$\psi_\tau = \left(I+\frac{\lambda}{\tau}(I-F(\tau))\right)^{-1}\phi \to \psi = (I+\lambda A)^{-1}\phi \tag{3.36}$$

for each $\phi\in\mathrm{L}^1$. Then

$$\lim_{n\to\infty} F\left(\frac{t}{n}\right)^n \phi = S(t)\phi \qquad \forall\phi\in\mathrm{L}^1. \qquad \square$$

4. Fully discrete relaxed scheme. In order to complete the description of the scheme, we need to specify the space discretization. We will use discretizations based on finite differences, in order to avoid cell coupling due to the source terms.

Note that the IMEX technique reduces the integration to a cascade of relaxation and transport steps. The former are the implicit parts of (3.5) and (3.7), while the transport steps appear in the evaluation of the explicit terms $B^{(i)}$ in (3.6). Since (3.5) and (3.7) involve only local operations, the main task of the space discretization is the evaluation of $\mathrm{div}(f)$, where we will exploit the linearity of f in its arguments.

4.1. One-dimensional scheme. Let us introduce a uniform grid on $[a,b]\subset\mathbb{R}$, $x_j = a-\frac{h}{2}+jh$ for $j=1,\dots,n$, where $h=(b-a)/n$ is the grid spacing and n the number of cells. The fully discrete scheme may be written as

$$z_j^{n+1} = z_j^n - \Delta t\sum_{i=1}^{\nu}\tilde{b}_i\left(F^{(i)}_{j+1/2}-F^{(i)}_{j-1/2}\right)+\frac{\Delta t}{\varepsilon}\sum_{i=1}^{\nu}b_i g(z_j^{(i)}), \tag{4.1}$$

where $F^{(i)}_{j+1/2}$ are the numerical fluxes, which are the only items we still need to specify. For convergence it is necessary to write the scheme in conservation form. Thus, following [34], we introduce the function $\hat{F}$ such that

$$f(z(x,t)) = \frac{1}{h}\int_{x-h/2}^{x+h/2} \hat{F}(s,t)\mathrm{d}s \quad \Rightarrow \frac{\partial f}{\partial x}(z(x_j,t)) = \frac{1}{h}\left(\hat{F}(x_{j+1/2},t) - \hat{F}(x_{j-1/2},t)\right).$$

The numerical flux function $F_{j+1/2}$ must approximate $\hat{F}(x_{j+1/2})$.

In order to compute the numerical fluxes, for each stage value, we reconstruct boundary extrapolated data $z^{(i)\pm}_{j+1/2}$ with a nonoscillatory interpolation method from the point values $z^{(i)}_j$ of the variables at the center of the cells. Next we apply a monotone numerical flux to these boundary-extrapolated data.

To minimize numerical viscosity we choose the Godunov flux, which in the present case of a linear system of equations reduces to the upwind flux. In order to select the upwind direction we write the system in characteristic form. The characteristic variables relative to the eigenvalues $\varphi, -\varphi, 0$ (in one space dimension φ reduces to a scalar parameter) are, respectively,

$$U = \frac{\varphi w + v}{2\varphi}, \qquad V = \frac{\varphi w - v}{2\varphi}, \qquad W = u - w. \tag{4.2}$$

Note that $u = U + V + W$. Therefore the numerical flux in characteristic variables is $F_{j+1/2} = (\varphi U^-_{j+1/2}, -\varphi V^+_{j+1/2}, 0)$.

The accuracy of the scheme depends on the accuracy of the reconstruction of the boundary-extrapolated data. For a first-order scheme we use a piecewise constant reconstruction such that $U^-_{j+1/2} = U_j$ and $V^+_{j+1/2} = V_{j+1}$. For higher-order schemes, we use ENO or WENO reconstructions of appropriate accuracy [35].

For $\varepsilon \to 0$ we obtain the relaxed scheme. Recall from (3.10) that the relaxation steps reduce to

$$w^{(i)}_j = p(u^{(i)}_j), \qquad v^{(i)}_j = -D\widehat{\nabla} w^{(i)}_j, \tag{4.3}$$

where $\widehat{\nabla}$ is a suitable approximation of the one-dimensional gradient operator. Thus the transport steps need to be applied only to $u^{(i)}$

$$u^{(i)}_j = u^n_j - \lambda \sum_{k=1}^{i-1} \tilde{a}_{i,k}\left[\varphi\left(U^{(k)-}_{j+1/2} - U^{(k)-}_{j-1/2}\right) - \varphi\left(V^{(k)+}_{j+1/2} - V^{(k)+}_{j-1/2}\right)\right]. \tag{4.4}$$

Finally, taking the last stage value and going back to conservative variables,

$$\begin{aligned} u^{n+1}_j = u^n_j - \frac{\lambda}{2}\sum_{i=1}^{\nu} \tilde{b}_i \Big(& [v^{(i)-}_{j+1/2} + v^{(i)+}_{j+1/2} - (v^{(i)-}_{j-1/2} + v^{(i)+}_{j-1/2})] \\ & + \varphi[w^{(i)-}_{j+1/2} - w^{(i)+}_{j+1/2} - (w^{(i)-}_{j-1/2} - w^{(i)+}_{j-1/2})]\Big). \end{aligned} \tag{4.5}$$

We wish to emphasize that the scheme reduces to the time advancement of the single variable u. Although the scheme is based on a system of three equations, the construction is used only to select the correct upwinding for the fluxes of the relaxed scheme, and the computational cost of each time step remains moderate.

4.2. Nonlinear stability for the first-order scheme. The relaxed scheme in the first-order case reduces to:

$$u_j^{n+1} = u_j^n + \frac{\lambda}{2}\left(\partial_x p(u^n)|_{j+1} - \partial_x p(u^n)|_{j-1}\right) + \frac{\lambda}{2}\varphi\left(p(u_{j+1}^n) - 2p(u_j^n) + p(u_{j-1}^n)\right). \tag{4.6}$$

We wish to compute the restrictions on λ and φ so that the scheme is total variation nonincreasing. We select the centered finite difference formula to approximate the partial derivatives of $p(u)$; we drop the index n and write p_j for $p(u_j^n)$. Define $\Delta_{j+1/2} = \frac{p_{j+1}-p_j}{u_{j+1}-u_j}$, and observe that these quantities are always nonnegative since p is nondecreasing. We obtain

$$\begin{aligned}
\mathrm{TV}(u^{n+1}) &= \sum_j |u_j^{n+1} - u_{j-1}^{n+1}| \\
&\le \sum_j \left\{ \frac{\lambda}{4h}\Delta_{j+3/2}|u_{j+2} - u_{j+1}| + \frac{\lambda}{2}\varphi\Delta_{j+1/2}|u_{j+1} - u_j| \right. \\
&\qquad + \left(1 - \lambda\left(\frac{1}{2h} + \varphi\right)\Delta_{j-1/2}\right)|u_j - u_{j-1}| \\
&\qquad \left. + \frac{\lambda}{2}\varphi\Delta_{j-3/2}|u_{j-1} - u_{j-2}| + \frac{\lambda}{4h}\Delta_{j-5/2}|u_{j-2} - u_{j-3}| \right\}
\end{aligned} \tag{4.7}$$

provided that

$$\left(1 - \lambda\left(\frac{1}{2h} + \varphi\right)\Delta_{j-1/2}\right) \ge 0 \qquad \forall j. \tag{4.8}$$

Assuming that the data have compact support, we can rescale all sums and finally get $\mathrm{TV}(u^{n+1}) \le \mathrm{TV}(u^n)$. Taking into account the Lipschitz condition on p, the scheme is total variation stable provided that (4.8) is satisfied, i.e., that

$$\Delta t \le \frac{2h^2}{\mu}\frac{1}{1+2h\varphi} \simeq \frac{(2-\delta)}{\mu}h^2, \tag{4.9}$$

where δ vanishes as h does. We point out that the stability condition is of the parabolic type. Finally, we observe that, using one-sided approximations for the partial derivatives of p in the scheme (4.6), one gets a stability condition involving the relation $\varphi > 1/h$. This would reintroduce in the scheme the constraint due to the stiffness in the convective term that prompted the introduction of φ in (2.3).

4.3. Linear stability. We study the linear stability of the schemes based on (4.3), (4.4), and (4.5) in the case when $p(u) = u$, by von Neumann analysis. We substitute the discrete Fourier modes $u_j^n = \rho^n e^{i(jk/N)}$ into the scheme, where k is the wave number and N the number of cells. We set $\xi = k/N$ and compute the amplification factor $Z(\xi)$ such that $u_j^{n+1} = Z(\xi)u_j^n$. We can consider ξ as a continuous variable, since the amplification factors for various choices of N all lie on the curves obtained considering the variable $\xi \in [0, 2\pi]$.

First we consider the same scheme studied in the previous section, for comparison purposes. Using piecewise constant reconstructions in space and forward Euler time integration, the amplification factor is $Z(\xi) = 1 + M(\xi)$, where

$$M(\xi) = \frac{\lambda}{h}\left(\cos(\xi) - 1\right)\left(\cos(\xi) + 1 + h\varphi\right).$$

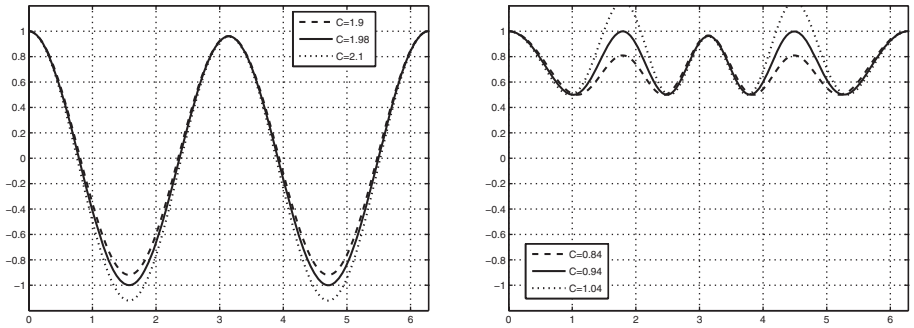

FIG. 4.1. *Amplification factor for upwind spatial reconstruction coupled with forward Euler (left) and for upwind second-order spatial reconstruction coupled with second-order time integration (right).*

$M(\xi)$ takes maximum value 0 and attains its minimum at the point ξ^* such that $\cos(\xi^*) = -\varphi h/2$. Stability requires that $M(\xi^*) \geq -2$, i.e.,

$$1 + \frac{\lambda}{h}\left(\frac{\varphi^2 h^2}{4} - 1\right) - \lambda\varphi\left(\frac{\varphi h}{2} + 1\right) \geq -1,$$

and, recalling that $\lambda = \Delta t/h$,

$$\Delta t \leq \frac{2h^2}{\left(1 + \frac{\varphi h}{2}\right)^2} \simeq 2\,(1 - \varphi h)\,h^2. \tag{4.10}$$

This gives a CFL condition of the form $\Delta t \leq 2(1-\delta)h^2$, where $\delta = O(h\varphi)$ (see Figure 4.1). These results are in very good agreement with those of the nonlinear analysis performed in the previous section.

Now we consider higher-order spatial reconstructions coupled with forward Euler time stepping. M takes the form

$$M(\xi, \gamma) = \frac{\lambda}{h}\left[f_1(\cos(\xi)) + \gamma f_2(\cos(\xi))\right],$$

where $\gamma = h\varphi$. Since γ is small, we compute the critical points ξ^* of $M(\xi, 0)$. For stability we thus require that $-2 \leq M(\xi^*, \gamma) \leq 0$.

We consider a piecewise linear and a WENO reconstruction. The first one is computed along characteristic variables using the upwind slope, while the gradient of $p(u)$ is computed with centered differences. The WENO reconstruction is fifth-order accurate and is obtained by setting to 1 the smoothness indicators, and the gradient of $p(u)$ is computed with the fourth-order centered difference formula.

For the piecewise linear reconstruction, we have that

$$M(\xi) = -\frac{\lambda}{h}\left[(\cos^2(\xi) - 1)(\cos(\xi) - 2) + h\varphi(\cos(\xi) - 1)^2\right],$$

and therefore

$$\Delta t \leq \frac{2h^2}{\frac{20+14\sqrt{7}}{27} + \frac{8+2\sqrt{7}}{9}\varphi h} \simeq 0.94(1 - 1.44\varphi h)h^2.$$

TABLE 4.1

	RK1	RK2	RK3
P-wise constant	2	2	2.51
P-wise linear	0.94	0.94	
WENO5	0.79	0.79	1

For the WENO reconstruction $M(\xi, \gamma)$ can be easily computed, and we get

$$\Delta t \leq 0.79(1 - 0.13\varphi h)h^2.$$

Now we wish to extend our results to the case of higher-order Runge–Kutta schemes. Since both the equation and the scheme are linear, the amplification factors for the Runge–Kutta schemes of orders 2 and 3 used here are, respectively,

$$Z_{(2)}(\xi) = 1 + M(\xi) + \frac{M(\xi)^2}{2},$$
$$Z_{(3)}(\xi) = 1 + M(\xi) + \frac{M(\xi)^2}{2} + \frac{M(\xi)^3}{6},$$

where $M(\xi)$ is the function appearing in the amplification factor relevant to the chosen spatial reconstruction. We have that

$$Z'_{(2)}(\xi) = M'(\xi)(1 + M(\xi)),$$
$$Z'_{(3)}(\xi) = M'(\xi)\left(1 + M(\xi) + \frac{M(\xi)^2}{2}\right),$$

and therefore the critical points are the points ξ^* such that $M'(\xi^*) = 0$.

In the Runge–Kutta 2 case the stability constraint $\|Z_{(2)}(\xi^*)\| \leq 1$ reduces to the CFL condition for the forward Euler scheme. For Runge–Kutta 3, $\|Z_{(3)}(\xi^*)\| \leq 1$, provided that

$$M(\xi^*) \geq \tilde{s} \simeq -2.51.$$

Notice that this is less restrictive than the Euler and second-order Runge–Kutta schemes for which the stability requirement is $M(\xi^*) \geq -2$.

For the third-order Runge–Kutta scheme with linearized WENO of order 5, we have

$$\Delta t \leq \frac{-\tilde{s}h^2}{2.51 + 0.33\varphi h} \simeq (1 - .1325\varphi h)h^2.$$

Table 4.1 summarizes the stability results obtained in this section by listing the values of the constant C that appears in the stability restriction $\Delta t \leq C(1 - C_1\varphi h)h^2$. Figures 4.1 and 4.2 contain the amplification factors $Z(\xi)$ for $\varphi = 1$ and $h = 10^{-2}$ for various choices of spatial reconstructions and time integration schemes. Each of them contains the curve corresponding to the value of C reported in Table 4.1 and two other close-by values.

4.4. Boundary conditions. Different boundary conditions can be implemented. Here we describe how to implement Neumann boundary conditions, considering for simplicity the one-dimensional case.

We first add g ghost points on each side of the computational domain $[a, b]$, where g depends on the order of the spatial reconstruction. We find a polynomial $q(x)$ of

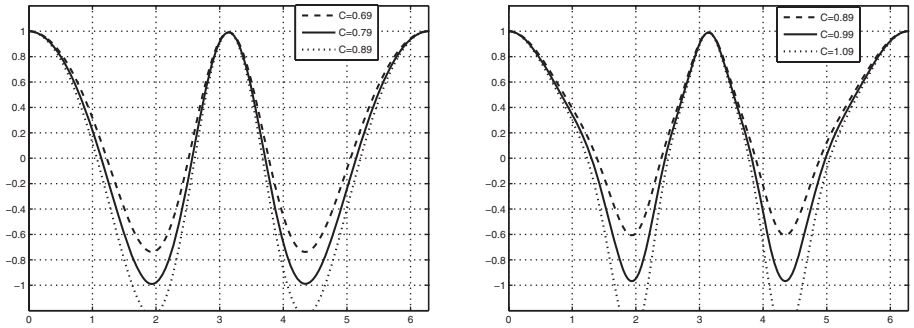

FIG. 4.2. *Amplification factors Z for WENO reconstructions of order* 5 *coupled with first-order (left) and third-order (right) time integration.*

degree d passing through the points (x_i, u_i) for $i = 1, \dots, d$ and having a prescribed derivative at the boundary point $x_{1/2} = a$. (The degree d is determined by the accuracy of the scheme that one wants to obtain and should match the degree of the reconstruction procedures used to obtain $U_j^{\pm}$ and $V_j^{\pm}$.) This polynomial is then used to set the values $u_{-i} = q(x_{-i})$ of the ghost points for $i = 0, 1, g-1$. One operates similarly at the right edge of the computational domain.

We also used periodic boundary conditions, which can be implemented with an obvious choice of the values u_i at the ghost points.

4.5. Multidimensional scheme. An appropriate numerical approximation of (2.3) in $\mathbb{R}^d$ that generalizes the scheme described in section 4.1 can be obtained by additive dimensional splitting. We consider the relaxed scheme, i.e., $\varepsilon = 0$, and for the sake of simplicity, let us focus on the square domain $[a, b] \times [a, b] \subset \mathbb{R}^2$. Here we shall describe the generalization of the scheme defined by (4.3), (4.2), (4.4), and (4.5) to the case of two space dimensions.

Without loss of generality, we consider a uniform grid in $[a, b] \times [a, b] \subset \mathbb{R}^2$ such that $\vec{x}_{i,j} = (x_i, y_j) = (a - h/2, a - h/2) + i(h, 0) + j(0, h)$ for $i, j = 1, 2, \dots, n$ and $h = (b - a)/n$.

In the present case, u and w are one-dimensional variables, while $\vec{v} = (v_{(1)}, v_{(2)})$ is now a field in $\mathbb{R}^2$. First we observe that the relaxation steps (4.3) are easily generalized for $d > 1$. For the transport steps, one has to evolve in time the system

$$\frac{\partial}{\partial t}\begin{pmatrix} u \\ v_{(1)} \\ v_{(2)} \\ w \end{pmatrix} + \frac{\partial}{\partial x}\begin{bmatrix} 0 & 1 & 0 & 0 \\ 0 & 0 & 0 & \varphi^2 \\ 0 & 0 & 0 & 0 \\ 0 & 1 & 0 & 0 \end{bmatrix}\begin{pmatrix} u \\ v_{(1)} \\ v_{(2)} \\ w \end{pmatrix} + \frac{\partial}{\partial y}\begin{bmatrix} 0 & 0 & 1 & 0 \\ 0 & 0 & 0 & 0 \\ 0 & 0 & 0 & \varphi^2 \\ 0 & 0 & 1 & 0 \end{bmatrix}\begin{pmatrix} u \\ v_{(1)} \\ v_{(2)} \\ w \end{pmatrix} = 0. \tag{4.11}$$

The semidiscretization in space of the above equation can be written as

$$\frac{\partial z_{i,j}}{\partial t} = -\frac{1}{h}\left(F_{i+1/2,j} - F_{i-1/2,j}\right) - \frac{1}{h}\left(G_{i,j+1/2} - G_{i,j-1/2}\right),$$

where F and G are the numerical fluxes in the x and the y direction, respectively, and can be written as

$$F_{i+1/2,j} = F(z^+_{i+1/2,j}, z^-_{i+1/2,j}), \qquad G_{i,j+1/2} = G(z^+_{i,j+1/2}, z^-_{i,j+1/2}).$$

The fluxes in the two directions are computed separately. We illustrate the computation of the flux F along the x direction. We note that only the field $v_{(1)}$ appears in

the differential operator along this direction. The third component of the flux is zero, and thus we have three independent characteristic variables, namely,

$$U_{(1)} = \frac{\varphi w + v_1}{2\varphi}, \qquad V_{(1)} = \frac{\varphi w - v_1}{2\varphi}, \qquad W = u - w,$$

which correspond, respectively, to the eigenvalues $\varphi, -\varphi, 0$. At this point the numerical fluxes can be easily evaluated by upwinding. We proceed similarly for the numerical flux G that depends on the characteristic variables $U_{(2)}, V_{(2)}, W$.

Denote by $U^{\pm}_{i+1/2,j}$ the reconstructions of $U_{(1)}(\cdot, y_j)$ at the point $(x_i + h/2, y_j)$. This involves a reconstruction of the restriction of $U_{(1)}$ to the line $y = y_i$ and can be obtained with any of the one-dimensional techniques mentioned in section 4.1. Similarly, denote by $U^{\pm}_{i,j+1/2}$ the reconstructions of $U_{(2)}(x_i, \cdot)$ at the point $(x_i, y_j + h/2)$. Now, (4.4) and (4.5) become, respectively,

$$u^{(l)}_{i,j} = u^n_{i,j} - \lambda \sum_{m=1}^{l-1} \tilde{a}_{l,m} \Big[\varphi\left(U^{(m)-}_{i+1/2,j} - U^{(m)-}_{i-1/2,j}\right) - \varphi\left(V^{(m)+}_{i+1/2,j} - V^{(m)+}_{i-1/2,j}\right) \varphi\left(U^{(m)-}_{i,j+1/2} - U^{(m)-}_{i,j-1/2}\right) - \varphi\left(V^{(m)+}_{i,j+1/2} - V^{(m)+}_{i,j-1/2}\right)\Big] \tag{4.12}$$

and

$$u^{n+1}_{i,j} = u^n_{i,j} - \lambda \sum_{l=1}^{\nu} \varphi \tilde{b}_l \Big[\left(U^{(l)-}_{i+1/2,j} - V^{(l)+}_{i+1/2,j}\right) - \left(U^{(l)-}_{i-1/2,j} - V^{(l)+}_{i-1/2,j}\right) \left(U^{(l)-}_{i,j+1/2} - V^{(l)+}_{i,j+1/2}\right) - \left(U^{(l)-}_{i,j-1/2} - V^{(l)+}_{i,j-1/2}\right)\Big]. \tag{4.13}$$

The generalization to $d > 2$ and rectangular domains is now trivial. We stress once again that no two-dimensional reconstruction is used, but only d one-dimensional reconstructions are needed. Finally, boundary conditions can be implemented directionwise with the same techniques used in the one-dimensional case.

5. Numerical results. We performed several numerical tests of our relaxed schemes. First we tested convergence for a linear diffusion equation with periodic and Neumann boundary conditions for initial data giving rise to smooth solutions. Next, numerical tests were also performed on the porous media equation $u_t = (u^m)_{xx}$, $m = 2, 3$, in both one and two dimensions.

5.1. Linear diffusion. For the first test we considered the linear problem

$$\begin{cases} \dfrac{\partial u}{\partial t}(x,t) = \dfrac{\partial^2 u}{\partial x^2} u(x,t), & x \in [0,1], \\ u(x,0) = u_0(x), & x \in [0,1]. \end{cases}$$

First we used periodic boundary conditions with $u_0(x) = \cos(2\pi x)$, so that $u(x,t) = \cos(2\pi x)e^{-4\pi^2 t}$ is an exact solution. Then we used Neumann boundary conditions $u_x(0) = u_x(1) = 1$ with initial data $u_0(x) = x + cos(2\pi x)$, so that $u(x,t) = x + \cos(2\pi x)e^{-4\pi^2 t}$ is an exact solution.

We tested the numerical schemes defined by (4.2), (4.3), (4.4), and (4.5) with various degrees of accuracy for the spatial reconstructions and time-stepping operators. We used ENO spatial reconstructions of degrees from 2 to 6 and WENO reconstructions of degrees 3 and 5. The time-stepping procedures chosen are IMEX

TABLE 5.1

L^1 *norms of the error and convergence rates for the linear diffusion equation with periodic boundary conditions, with smooth initial data.*

	$N = 40$	$N = 80$	$N = 160$	$N = 320$	$N = 640$
ENO2, RK1	2.012e-03	5.6378e-04	1.0736e-04	1.5539e-05	2.5065e-06
ENO3, RK2	1.9066e-06	2.3057e-07	5.6115e-08	8.6904e-09	1.1905e-09
ENO4, RK2	7.7517e-06	5.7082e-07	3.3507e-08	1.4978e-09	7.0725e-11
ENO5, RK3	1.3864e-08	6.0259e-10	2.2121e-11	7.4454e-13	2.3803e-14
ENO6, RK3	1.5538e-08	8.5661e-10	1.446e-11	1.7111e-13	1.5311e-15
WENO3, RK2	1.9799e-03	5.1278e0-4	1.4332e-04	2.1488e-05	7.512e-08
WENO5, RK3	1.5892e-07	4.8069e-09	1.59e-10	5.2337e-12	1.6758e-13

	$N = 40$	$N = 80$	$N = 160$	$N = 320$	$N = 640$
ENO2, RK1	1.3973	1.8354	2.3926	2.7886	2.6322
ENO3, RK2	5.9501	3.0477	2.0388	2.6909	2.8678
ENO4, RK2	3.8987	3.7634	4.0905	4.4836	4.4045
ENO5, RK3	6.8124	4.524	4.7677	4.8929	4.9671
ENO6, RK3	5.9907	4.181	5.8885	6.401	6.8043
WENO3, RK2	0.56648	1.949	1.8391	2.7376	8.1601
WENO5, RK3	2.9595	5.0471	4.918	4.925	4.9649

TABLE 5.2

L^1 *norms of the error and convergence rates for the linear diffusion equation with Neumann boundary conditions, with smooth initial data.*

	$N = 40$	$N = 80$	$N = 160$	$N = 320$	$N = 640$
ENO2, RK1	2.1965e-03	5.7152e-04	1.4301e-04	2.32e-05	4.743e-06
ENO3, RK2	2.0621e-06	2.2641e-07	6.7935e-08	8.8255e-09	1.2339e-09
ENO4, RK2	8.1764e-06	5.4431e-07	3.6974e-08	1.3686e-09	8.335e-11
ENO5, RK3	1.5484e-07	4.4163e-09	1.2405e-10	3.7803e-12	1.1669e-13
WENO3, RK2	1.9092e-03	4.4225e-04	1.2914e-04	4.5037e-06	7.4526e-08
WENO5, RK3	2.5048e-07	4.9279e-09	1.4776e-10	4.7482e-12	1.4948e-13

	$N = 40$	$N = 80$	$N = 160$	$N = 320$	$N = 640$
ENO2, RK1	1.4361	1.9424	1.9987	2.624	2.2902
ENO3, RK2	6.1004	3.1871	1.7367	2.9444	2.8385
ENO4, RK2	3.9763	3.909	3.8798	4.7558	4.0373
ENO5, RK3	5.6626	5.1317	5.1539	5.0362	5.0178
WENO3, RK2	1.2624	2.11	1.7759	4.8417	5.9172
WENO5, RK3	4.9122	5.6676	5.0597	4.9597	4.9893

Runge–Kutta schemes of section 3 of accuracy chosen to match the accuracy of the spatial reconstruction. Since stability forces the parabolic restriction $\Delta t \leq Ch^2$, an IMEX scheme of order m was coupled with a spatial ENO/WENO reconstruction of accuracy p such that $p \leq 2m$, obtaining a scheme of order p.

We computed the numerical solution of the diffusion equation with final time $t = 0.05$ with $N = 40, 80, 160, 320, 640$ grid points and computed the L^1 norm of the difference between the numerical and the exact solution. The results are in Table 5.1 for the periodic boundary conditions and Table 5.2 for the Neumann boundary conditions. One can see that the expected convergence rates are reached, even if the combination of the WENO reconstruction of accuracy 3 and the IMEX scheme of second order reach the predicted error reduction only on very fine grids.

5.2. Porous media equation. On the porous media equation (1.1) with $p(u) = u^m$ we performed a test proposed in [18]. We took $m = 2, 3$ and initial data of class

TABLE 5.3
L^1 *norms of the error and convergence rates for the porous media equation periodic boundary conditions, with initial data of class* C^1.

	$N = 60$	$N = 180$	$N = 540$	$N = 1620$
ENO2, RK1	2.6365e-04	1.9898e-05	2.049e-06	2.076e-07
ENO3, RK2	1.9605e-05	6.0423e-07	2.4141e-08	8.9729e-10
ENO4, RK2	1.2127e-05	2.967e-07	9.9925e-09	3.5781e-10
ENO5, RK3	4.694e-06	1.719e-07	6.3248e-09	2.4447e-10
ENO6, RK3	4.1099e-06	1.4711e-07	5.3992e-09	2.0849e-10
WENO3, RK2	1.5871e-04	1.0448e-05	4.3463e-07	8.8767e-09
WENO5, RK3	7.5662e-06	4.6049e-07	7.4746e-09	2.7985e-10

	$N = 60$	$N = 180$	$N = 540$	$N = 1620$
ENO2, RK1	2.8243	2.352	2.0692	2.084
ENO3, RK2	5.1899	3.1672	2.931	2.9968
ENO4, RK2	5.6271	3.3774	3.0865	3.0307
ENO5, RK3	6.491	3.0103	3.006	2.9611
ENO6, RK3	6.612	3.0311	3.0083	2.962
WENO3, RK2	3.2863	2.4765	2.8942	3.5418
WENO5, RK3	6.0565	2.5479	3.7509	2.9902

C^1 as follows:

$$u(x,0) = \begin{cases} \cos^2(\pi x/2), & |x| \le 1, \\ 0, & |x| > 1. \end{cases} \tag{5.1}$$

The computational domain is $\{|x| \le 3\} \subset \mathbb{R}$, and the boundary conditions are periodic; the CFL constant is taken as $C = 0.25$.

Since the initial data have compact support and are Lipschitz continuous, the solution will be of compact support for every $t \ge 0$ but will develop a discontinuity in u_x at some finite time $\tau > 0$ (see [3]).

As was shown in [3], the solution with the initial condition we chose has a front that does not move for $t < 0.034$. We therefore chose a final time of the simulation $t_{\text{fin}} = 0.03$ to prevent the formation of the singularity of u_x from affecting the order of convergence. We used as a reference solution the one obtained numerically with $N = 4860$ grid points and computed the L^1 norms of the errors of the solutions with $N = 60, 180, 540, 1620$ grid points. The results are presented in Table 5.3.

First of all one verifies that the degree of regularity of the solution poses a limit on the order of convergence of the schemes: Therefore the schemes we tested perform at best as third-order schemes, as confirmed by the data in Table 5.3. Still, high-order schemes yield a smaller error on a given grid. This can be of practical importance in problems where one does not have the freedom of choosing the number of grid points, as in digital image analysis, where nonlinear degenerate diffusion equations are sometimes used as filters for contour enhancement (see [5]).

In Figure 5.1 we show the numerical solution for the porous media equation with $p(u) = u^2$ and $p(u) = u^3$, with the initial data (5.1) and $t \in [0, 2]$. It can be appreciated that a front (i.e., a discontinuity of $\frac{\partial u}{\partial x}$) develops at a finite time and then it travels at finite speed.

We present a numerical simulation for the two-dimensional porous media equation (1.1) with $p(u) = u^2$. We chose an initial data $u_0(x, y)$ given by two bumps with periodic boundary conditions on $[-10, 10] \times [-10, 10]$. The large domain ensures that the compact support of the solution is still contained in the computational domain

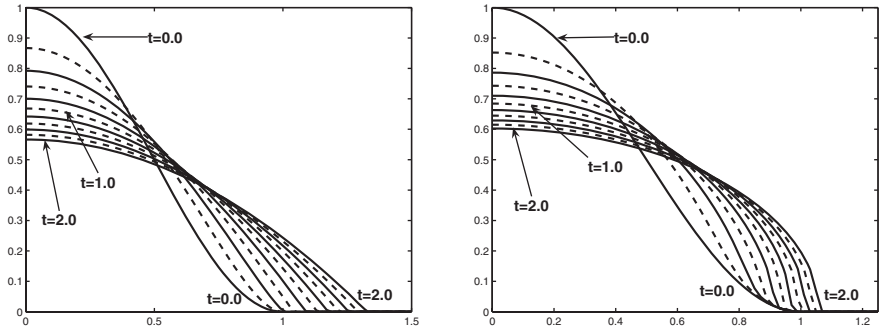

FIG. 5.1. *Snapshots of the numerical solutions for the porous media equation with* $p(u) = u^2$ *(left) and* $p(u) = u^3$ *(right). Initial data are chosen according to* (5.1)*, and the numerical solutions are represented at times* $t = 0, 0.2, \ldots, 2.0$*. The solutions are obtained with the spatial WENO reconstruction of order* 5 *and the RK*3 *time integrator.*

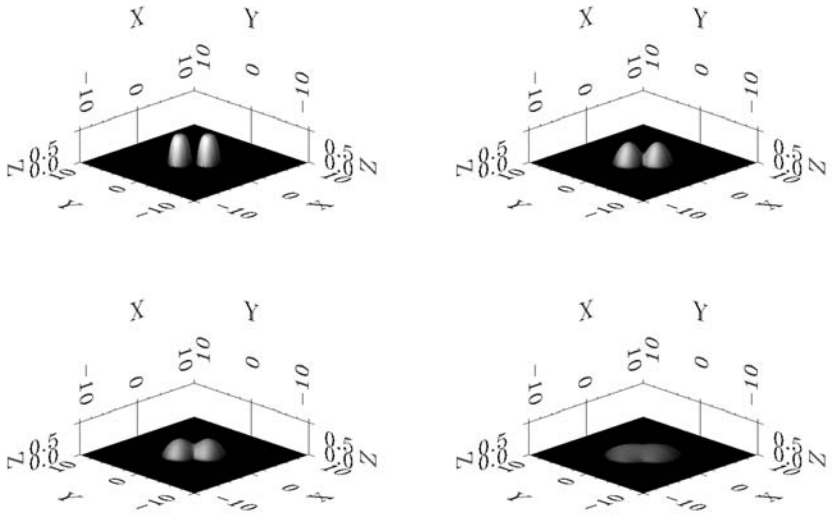

FIG. 5.2. *The numerical solution of the porous media equation on a square regular grid with compactly supported initial data. From top left to bottom right, we show the numerical solution at times* $t = 0, 0.5, 1.0, 4.0$*.*

at the final time of the calculation. The numerical approximation at different time levels is shown in Figure 5.2.

We can note that the symmetries of the initial data are preserved and the solution seems to be unaffected by the dimensional splitting of the two-dimensional scheme.

6. Conclusions. We have proposed and analyzed relaxed schemes for nonlinear degenerate parabolic equations.

We considered a relaxation system similar to the one used in [29, 27] but focused on the relaxed schemes that are obtained by taking the relaxation parameter $\varepsilon = 0$. By using suitable discretizations in space and time, namely, ENO/WENO nonoscillatory reconstructions for numerical fluxes and IMEX Runge–Kutta schemes for time

integration, we have obtained a class of high-order schemes. We proved a convergence theorem for the semidiscrete scheme using the nonlinear Chernoff formula; furthermore we obtained stability results for the fully discrete schemes. Our computational tests suggest that our schemes converge with the predicted rate and exhibit a high resolution of propagating fronts.

Finally, we point out that these schemes can be easily implemented on parallel computers. Some preliminary results and details are reported in [12]. In particular the schemes involve only linear matrix-vector operations, and the execution time scales linearly when increasing the number of processors.

Our numerical approach can be easily extended to more general problems. The case of degenerate reaction-diffusion equations will appear in [13]. The treatment of convection-diffusion equations requires the introduction of an additional equation to relax the convection terms. A preliminary study appears in [9], while some of these applications will appear in a forthcoming paper [11].

REFERENCES

[1] D. Aregba-Driollet, R. Natalini, and S. Tang, *Explicit diffusive kinetic schemes for nonlinear degenerate parabolic systems*, Math. Comp., 73 (2004), pp. 63–94.

[2] D. Aregba-Driollet and R. Natalini, *Discrete kinetic schemes for multidimensional systems of conservation laws*, SIAM J. Numer. Anal., 37 (2000), pp. 1973–2004.

[3] D. G. Aronson, *Regularity properties of flows through porous media: A counterexample*, SIAM J. Appl. Math., 19 (1970), pp. 299–307.

[4] U. Asher, S. Ruuth, and R. Spiteri, *Implicit-explicit Runge-Kutta methods for time dependent partial differential equations*, Appl. Numer. Math., 25 (1997), pp. 151–167.

[5] G. I. Barenblatt and J. L. Vázquez, *Nonlinear diffusion and image contour enhancement*, Interfaces Free Bound., 6 (2004), pp. 31–54.

[6] A. Berger, H. Brezis, and J. Rogers, *A numerical method for solving the problem $u\_t - \Delta f(u) = 0$*, RAIRO Numer. Anal., 13 (1979), pp. 297–312.

[7] F. Bouchut, F. R. Guarguaglini, and R. Natalini, *Diffusive BGK approximations for nonlinear multidimensional parabolic equations*, Indiana Univ. Math. J., 49 (2000), pp. 723–749.

[8] H. Brézis and A. Pazy, *Convergence and approximation of semigroups of nonlinear operators in Banach spaces*, J. Funct. Anal., 9 (1972), pp. 63–74.

[9] F. Cavalli, G. Naldi, G. Puppo, and M. Semplice, *A comparison between relaxation and Kurganov-Tadmor schemes*, in Progress in Industrial Mathematics at ECMI 2006, L. L. Bonilla, M. Moscoso, G. Platero, and J. M. Vega, eds., Mathematics in Industry 12, Springer, 2007.

[10] F. Cavalli, G. Naldi, G. Puppo, and M. Semplice, *Increasing efficiency through optimal RK time integration of diffusion equations*, in Proceedings of the HYP2006 Conference, 2006, to appear.

[11] F. Cavalli, G. Naldi, G. Puppo, and M. Semplice, *High Order Relaxation Approximation of Convection Diffusion Equations*, manuscript.

[12] F. Cavalli, G. Naldi, and M. Semplice, *Parallel algorithms for nonlinear diffusion by using relaxation approximation*, in ENUMATH 2005, A. Bermúdez de Castro, D. Gómez, P. Quintela, and P. Salgado, eds., Springer, Berlin, 2006, pp. 404–411.

[13] F. Cavalli and M. Semplice, *High order relaxed schemes for nonlinear reaction diffusion problems*, in Proceedings of the SIMAI 2006 Conference, 2006, submitted.

[14] M. Crandall and T. Liggett, *Generation of semi-groups of non linear transformations on general Banach spaces*, Amer. J. Math., 93 (1971), pp. 265–298.

[15] M. S. Espedal and K. H. Karlsen, *Numerical solution of reservoir flow models based on large time step operator splitting algorithms*, in Filtration in Porous Media and Industrial Application (Cetraro, 1998), Lecture Notes in Math. 1734, Springer, Berlin, 2000, pp. 9–77.

[16] S. Evje and K. H. Karlsen, *Viscous splitting approximation of mixed hyperbolic-parabolic convection-diffusion equations*, Numer. Math., 83 (1999), pp. 107–137.

[17] S. Gottlieb, C.-W. Shu, and E. Tadmor, *Strong stability-preserving high-order time discretization methods*, SIAM Rev., 43 (2001), pp. 89–112.

[18] J. L. Graveleau and P. Jamet, *A finite difference approach to some degenerate nonlinear parabolic equations*, SIAM J. Appl. Math., 20 (1971), pp. 199–223.
[19] W. Jäger and J. Kačur, *Solution of porous medium type systems by linear approximation schemes*, Numer. Math., 60 (1991), pp. 407–427.
[20] S. Jin and C. D. Levermore, *Numerical schemes for hyperbolic conservation laws with stiff relaxation terms*, J. Comput. Phys., 126 (1996), pp. 449–467.
[21] S. Jin, L. Pareschi, and G. Toscani, *Diffusive relaxation schemes for multiscale discrete-velocity kinetic equations*, SIAM J. Numer. Anal., 35 (1998), pp. 2405–2439.
[22] S. Jin and Z. Xin, *The relaxation schemes for systems of conservation laws in arbitrary space dimensions*, Comm. Pure Appl. Math., 48 (1995), pp. 235–276.
[23] J. Kačur, A. Handlovičová, and M. Kačurová, *Solution of nonlinear diffusion problems by linear approximation schemes*, SIAM J. Numer. Anal., 30 (1993), pp. 1703–1722.
[24] C. Lattanzio and R. Natalini, *Convergence of diffusive BGK approximations for nonlinear strongly parabolic systems*, Proc. Roy. Soc. Edinburgh Sect. A, 132 (2002), pp. 341–358.
[25] P. Lions and G. Toscani, *Diffusive limit for two-velocity Boltzmann kinetic models*, Rev. Mat. Iberoamericana, 13 (1997), pp. 473–513.
[26] E. Magenes, R. H. Nochetto, and C. Verdi, *Energy error estimates for a linear scheme to approximate nonlinear parabolic problems*, RAIRO Modél. Math. Anal. Numér., 21 (1987), pp. 655–678.
[27] G. Naldi, L. Pareschi, and G. Toscani, *Relaxation schemes for partial differential equations and applications to degenerate diffusion problems*, Surv. Math. Indust., 10 (2002), pp. 315–343.
[28] G. Naldi and L. Pareschi, *Numerical schemes for kinetic equations in diffusive regimes*, Appl. Math. Lett., 11 (1998), pp. 29–35.
[29] G. Naldi and L. Pareschi, *Numerical schemes for hyperbolic systems of conservation laws with stiff diffusive relaxation*, SIAM J. Numer. Anal., 37 (2000), pp. 1246–1270.
[30] R. H. Nochetto, A. Schmidt, and C. Verdi, *A posteriori error estimation and adaptivity for degenerate parabolic problems*, Math. Comp., 69 (2000), pp. 1–24.
[31] R. H. Nochetto and C. Verdi, *Approximation of degenerate parabolic problems using numerical integration*, SIAM J. Numer. Anal., 25 (1988), pp. 784–814.
[32] L. Pareschi and G. Russo, *Implicit-explicit Runge-Kutta schemes and applications to hyperbolic systems with relaxation*, J. Sci. Comput., 25 (2005), pp. 129–155.
[33] I. S. Pop and W. Yong, *A numerical approach to degenerate parabolic equations*, Numer. Math., 92 (2002), pp. 357–381.
[34] C. Shu and S. Osher, *Efficient implementation of essentially nonoscillatory shock-capturing schemes.* II, J. Comput. Phys., 83 (1989), pp. 32–78.
[35] C. Shu, *Essentially non-oscillatory and weighted essentially non-oscillatory schemes for hyperbolic conservation laws*, in Advanced Numerical Approximation of Nonlinear Hyperbolic Equations (Cetraro, 1997), Lecture Notes in Math. 1697, Springer, Berlin, 1998, pp. 325–432.
[36] J. L. Vázquez, *An introduction to the mathematical theory of the porous medium equation*, in Shape Optimization and Free Boundaries (Montreal, PQ, 1990), NATO Sci. Ser. C Math. Phys. Sci. 380, Kluwer Academic Publishers, Dordrecht, 1992, pp. 347–389.
[37] J. Weickert, *Anisotropic Diffusion in Image Processing*, European Consortium for Mathematics in Industry, B. G. Teubner, Stuttgart, 1998.